THE JOURNAL OF BIOLOGICAL CHEMISTRY VOL. 281, NO. 40, pp. 29669–29674, October 6, 2006

RGS2 Inhibits the Epithelial Ca^{2+} Channel TRPV6*

Received for publication, June 29, 2006, and in revised form, August 7, 2006 Published, JBC Papers in Press, August 8, 2006, DOI 10.1074/jbc.M606233200

Joost P. Schoeber[‡], Catalin N. Topala[‡], Xinhua Wang[§], Robin J. Diepens[‡], Tim T. Lambers[‡], Joost G. Hoenderop[‡], and René J. Bindels[‡1]

From the [‡]Department of Physiology, Nijmegen Centre for Molecular Life Sciences, Radboud University Nijmegen Medical Centre, Nijmegen 6500 HB, The Netherlands and the [§]Department of Physiology, University of Texas Southwestern Medical Center, Dallas, Texas 75390-9040

The epithelial Ca^{2+} channels TRPV5 and TRPV6 constitute the apical Ca^{2+} entry pathway in the process of active Ca^{2+} (re)absorption. By yeast two-hybrid and glutathione *S*-transferase pulldown analysis we identified RGS2 as a novel TRPV6-associated protein. RGS proteins determine the inactivation kinetics of heterotrimeric G-protein-coupled receptor (GPCR) signaling by regulating the GTPase activity of G_α subunits. Here we demonstrate that TRPV6 interacts with the NH_2-terminal domain of RGS2 in a Ca^{2+}-independent fashion and that overexpression of RGS2 reduces the Na^+ and Ca^{2+} current of TRPV6 but not that of TRPV5-transfected human embryonic kidney 293 (HEK293) cells. In contrast, overexpression of the deletion mutant ΔN-RGS2, lacking the NH_2-terminal domain of RGS2, in TRPV6-expressing HEK293 cells did not show this inhibition. Furthermore, cell surface biotinylation indicated that the inhibitory effect of RGS2 on TRPV6 activity is not mediated by differences in trafficking or retrieval of TRPV6 from the plasma membrane. This effect probably results from the direct interaction between RGS2 and TRPV6, affecting the gating properties of the channel. Finally, the scaffolding protein spinophilin, shown to recruit RGS2 and regulate GPCR-signaling via G_α, did not affect RGS2 binding and electrophysiological properties of TRPV6, indicating a GPCR-independent mechanism of TRPV6 regulation by RGS2.

The transient receptor potential (TRP)[2] superfamily includes more than 30 different proteins, all of which are considered to form subunits of cation channels (1–5). Based on sequence homology, the TRP family can be divided in seven main subfamilies: the TRPC ("canonical") family, the TRPV ("vanilloid") family, the TRPM ("melastatin") family, the TRPP ("polycystin") family, the TRPML ("mucolipin") family, the TRPA ("ankyrin") family, and the TRPN ("NOMPC") family. TRPV6 is the most Ca^{2+}-selective ion channel in the TRP superfamily with a Ca^{2+} selectivity of more than 100 times over monovalent cations (6, 7).

Recently, the electrophysiological properties of TRPV6 have been studied extensively. When measured in heterologous expression systems, TRPV6 displays characteristic inward rectifying currents carried by Ca^{2+} or monovalent cations when Ca^{2+} is omitted from the extracellular solution. These inward currents are blocked by Mg^{2+} in a voltage-dependent manner (8), which is removed upon neutralization of a single negatively charged amino acid residue, Asp^{541}, within the pore region. The pore diameter of TRPV6 was recently estimated at 5.4 Å by cystein scanning experiments (9). Together with its closest relative, TRPV5, TRPV6 shares a common feature that is the Ca^{2+}-dependent inactivation of the currents.

TRPV6 is predominantly expressed in placenta, pancreas, small intestine, and colon (6, 10–12). In these tissues TRPV6 plays a major role in Ca^{2+} transport (reviewed in Refs. 13 and 14).

To date, screening and domain mapping of the carboxyl terminus of TRPV6 has revealed proteins associating with TRPV6 and subsequently the regulatory functions of these interacting proteins have been studied, *e.g.* Rab11a, NHERF4, S100A10 (15–17). In contrast, little is known about the molecular mechanisms involved in regulation of the channel via its intracellular NH_2-terminal domain. At present, six ankyrin repeats have been predicted in this region (18). Ankyrin repeats have been shown to act as a scaffold in molecular recognition to mediate protein-protein interactions (19). These, or other regions in the NH_2-terminal domain of TRPV6, may bind regulatory proteins interacting in pathways that mediate the Ca^{2+}-transporting activity of the channel.

The aim of this study was to identify regulatory proteins that interact with the NH_2-terminal domain of TRPV6. To this end, we identified RGS2 as a novel binding partner of TRPV6 by yeast two-hybrid screening. RGS2 is a member of the RGS family of proteins that are able to terminate signaling of heterotrimeric G-protein-coupled receptors (GPCRs) by enhancing the GTPase activity of active G_α subunits (20). To date, over 20 different RGS proteins have been identified, and their effector functions extend beyond negative regulation of GPCR signaling. RGS proteins can act as effector antagonists, binding to either the effector protein or the G_α subunit to prevent an operative physical interaction. They have also been shown to interact with a wide variety of auxiliary proteins, such as calmodulin, spinophilin (SPL), and 14-3-3 protein, which can influence their subcellular localization, stability, and function (21). In this respect, the finding of RGS2 as a protein interacting with TRPV6 may lead to altered channel activity by disturbances in protein trafficking or a direct effect at the cell surface. The

* This work was supported by the Dutch Organization of Scientific Research (NWO-ALW 814.02.001 and Zon-MW 016.006.001). The costs of publication of this article were defrayed in part by the payment of page charges. This article must therefore be hereby marked "*advertisement*" in accordance with 18 U.S.C. Section 1734 solely to indicate this fact.

[1] To whom correspondence should be addressed. E-mail: R.Bindels@ncmls.ru.nl.

[2] The abbreviations used are: TRP, transient receptor potential; GPCR, G-protein-coupled receptor; SPL, spinophilin; HA, hemagglutinin; ENaC, epithelial Na^+ channel; RT, reverse transcriptase; GST, glutathione *S*-transferase; HEK, human embryonic kidney; DVF, divalent-free.

putative role of RGS2 in active Ca^{2+} absorption was established by a comprehensive approach including pulldown assays, electrophysiological analysis, and cell-surface expression of RGS2 interacting with TRPV6.

EXPERIMENTAL PROCEDURES

Constructs and cRNA Synthesis—The TRPV6, TRPV6 N-tail, and TRPV5 constructs were generated in pGEX 6p-2 and pCINeo/IRES-GFP vectors as described previously (22). The coding sequence of wild-type RGS2 protein was amplified from total mouse kidney cDNA material using primers with a HA tag included and cloned into the PT7Ts vector as BglII-SpeI fragment, and subsequently into the pCINeo/IRES-GFP vector as an NheI-XhoI fragment. RGS2 and ΔN-RGS2 (deletion of the NH_2-terminal domain of RGS2: amino acids 1–82) were subcloned from the PT7Ts vector without the HA tag to the pGEX 6p-2 (Amersham Biosciences) vector using forward and reverse primers containing BamHI and XhoI restriction sites, respectively. pT7Ts constructs were linearized, and cRNA was synthesized *in vitro* as described previously (16). In pCINeo/IRES-GFP, ΔN-RGS2 was obtained by *in vitro* mutagenesis of wild-type RGS2. All constructs were verified by sequence analysis. Rat-SPL (in pCMV-myc) and human-RGS2 (in pGex-KG) constructs were described previously (23).

Yeast Two-hybrid System—Yeast-two-hybrid experiments were performed as described previously (16). In short, the N-tail of mouse TRPV6 was cloned in the pAS-1 yeast cloning and expression vector. Using this vector, the yeast strain Y153 was transformed to Trp prototrophy. Subsequently, yeast was transformed with a mouse kidney cDNA library (Clontech, Palo Alto, CA) present in the pACT2 vector, containing a leucine selection marker. Yeast cells were plated on Trp-Leu-His-selective medium containing 25 mM 3-aminotriazole. Positive colonies were assayed for β-galactosidase activity. Subsequently, yeast DNA of positive colonies was isolated, and prey plasmids were rescued by electroporation into KC8 cells. Results were confirmed using purified library plasmids, and a negative control was performed by replacing the pAS-1 containing the N-tail of mouse TRPV6 with the pAS-1 containing the N-tail of rat γ-subunit of the epithelial Na^+ channel (ENaC).

Reverse Transcriptase (RT)-PCR Analysis—Total RNA was isolated from different mouse tissues using TRIzol and subjected to reverse transcription as described (24). For RGS2 RT-PCR, the oligonucleotide primer sequences were as follows: forward primer with BglII restriction site, 5′-GAAGATCTGCCACCATGCAAAGTGCCAGTTCCTG-3′; reverse with SpeI restriction site, 5′-GGACTAGTTCATGTAGCATGGGGCTCCG-3′; β-actin, 5′-ACGATTTCCCTCTCAGCTGTG-3′ (forward) and 5′-GTATGCCTCTGGTCGTACCAC-3′ (reverse). For SPL the following primers were used: forward primer, 5′-CTTAGGAACACCAAAGGCC-3′; reverse primer, 5′-GTAGTCCTTGATGAGACGC-3′. PCR fragments were analyzed by electrophoresis on 1% (w/v) agarose.

Pulldown Assays—RGS2 pGex-KG and HA-RGS2, HA-ΔN-RGS2, and empty pGex 6p-2 constructs were transformed in *Escherichia coli* BL21 and glutathione *S*-transferase (GST) fusion proteins were expressed and purified according to the manufacturer's protocol (Amersham Biosciences). [^{35}S]Methionine-labeled TRPV6 N-tail was prepared using a reticulocyte lysate system (Promega, Madison, WI) and analyzed for pulldown with GST, GST-HA-RGS2, or GST-HA-ΔN-RGS2 fusion proteins immobilized on glutathione-Sepharose 4B beads (Amersham Biosciences) as described previously (16). After extensive washing, bound proteins were subjected to SDS-PAGE, and visualized by Coomassie staining and autoradiography. For pulldown with hRGS2, TRPV6/mock, SPL/mock, and TRPV6/SPL were transiently transfected in human embryonic kidney 293 (HEK293) cells and after 72-h extracts from lysed cells were adjusted to equal input concentrations and analyzed for pulldown with GST or GST-hRGS2 fusion proteins immobilized on gluthatione-Sepharose 4B beads. The beads were washed extensively and pulled proteins were analyzed by SDS-PAGE and immunoblotting.

Electrophysiology and Solutions—The full-length cDNAs encoding TRPV5, TRPV6, RGS2, and ΔN-RGS2 were transiently transfected in HEK293 cells and patch clamp experiments were performed in the tight-seal whole-cell configuration at room temperature using an EPC-9 patch clamp amplifier controlled by the Pulse software (HEKA Elektronik, Lambrecht, Germany), as described previously (25). Cells were held at 20 mV, and voltage ramps of 450 ms, ranging from −100 to +100 mV, were applied every 5 s. Cell capacitance and access resistance were monitored continuously using the automatic capacitance compensation of the Pulse software. Na^+ current densities were obtained by dividing the current amplitude measured at −80 mV during the ramp protocols by the cell capacitance. Ca^{2+}-dependent inactivation was studied using a 3-s voltage step to −100 mV from a holding potential of +70 mV. From this step protocol, Ca^{2+} peak values were extracted by dividing the current at −100 mV by the cell capacitance. The standard extracellular solution (Krebs) contained: 150 mM NaCl, 6 mM CsCl, 1 mM $MgCl_2$, 10 mM HEPES/NaOH, and 10 mM glucose, pH 7.4. The concentration of Ca^{2+} ranged between 1 and 10 mM. Divalent-free (DVF) solutions did not contain added divalent cations, whereas trace amounts of divalent cations were removed with 100 μM EDTA. The standard internal (pipette) solution contained: 20 mM CsCl, 100 mM Cs-aspartate, 1 mM $MgCl_2$, 4 mM Na_2ATP, 10 mM BAPTA, 10 mM HEPES/CsOH, pH 7.2. Cells were kept in a nominal Ca^{2+}-free medium to prevent Ca^{2+} overload and exposed for a maximum of 5 min to a Krebs solution containing 1.5 mM Ca^{2+} before sealing the patch pipette to the cell. The analysis and display of patch clamp data were performed using Igor Pro software (WaveMetrics, Lake Oswego, OR).

Biotinylation—TRPV6, HA-RGS2, and empty pCINeo/IRES-GFP constructs were transfected transiently in HEK293 cells and subjected to cell surface biotinylation as described previously (26). Biotinylated proteins were eluted with SDS-PAGE loading buffer, separated on 10% (w/v) SDS-PAGE gel, and analyzed by immunoblotting with rabbit antiserum against TRPV6 (1:2000) (11).

Statistical Analysis—In all experiments, the data are expressed as mean ± S.E. Overall statistical significance was determined by analysis of variance. In case of significance ($p < 0.05$), individual groups were compared using a Student's *t* test.

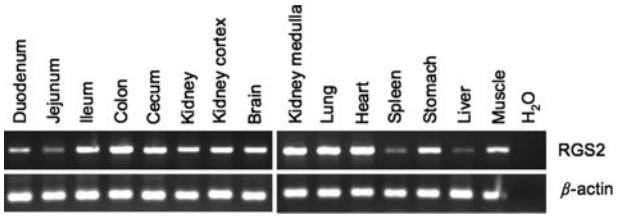

FIGURE 1. **Tissue distribution of RGS2.** RNA was extracted from different mouse tissues and RGS2 expression was determined by RT-PCR. The RGS2-specific band was amplified from all the indicated tissues (*upper panel*). As a control, β-actin was amplified to ensure the integrity of the cDNAs (*lower panel*).

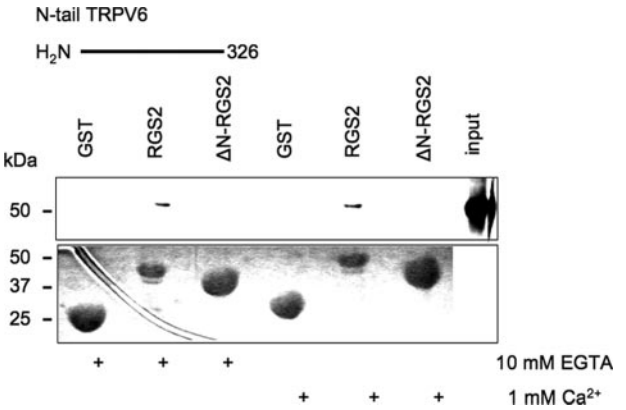

FIGURE 2. **Interaction of TRPV6 and RGS2.** [^{35}S]Methionine-labeled TRPV6 N-tail was incubated with GST, GST/RGS2, or GST/ΔN-RGS2 immobilized on glutathione-Sepharose 4B beads, either in the presence (1 mM Ca^{2+}) or absence (10 mM EGTA) of Ca^{2+}. TRPV6 N-tail interacted with RGS2, whereas no binding with GST/ΔN-RGS2 or GST alone was observed.

RESULTS

Identification of RGS2 as a TRPV6-associated Protein—To identify proteins that interact with TRPV6, the NH_2-terminal tail of TRPV6 was used to screen a library of mouse kidney cDNA by the yeast two-hybrid technique. RGS2 was identified as a positive clone and belongs to the R4 subfamily of regulator of G-protein signaling proteins (27). To confirm the interaction, the full-length cDNA sequence of RGS2 was re-analyzed in a yeast two-hybrid with the N-tail of TRPV6 as bait. The γ-subunit of the epithelial Na^+ channel (γENaC) was used as a negative control. TRPV6 and RGS2 displayed a strong interaction, whereas TRPV6 and γENaC did not interact (data not shown).

The RGS2 Gene Is Ubiquitously Expressed—The expression of RGS2 in different mouse tissues was analyzed by RT-PCR. RGS2 was detected ubiquitously (Fig. 1, *upper panel*). All tissues expressed β-actin that was used as a positive control to confirm the integrity of the cDNAs (Fig. 1, *lower panel*). As negative controls, the primer sets for RGS2 and β-actin were screened in the absence of cDNA (depicted as H_2O samples in Fig. 1).

TRPV6 Interacts with the NH_2-terminal Domain of RGS2—The interaction between TRPV6 and the binding domain of RGS2 was further established using GST pulldown assays. To this end, RGS2 and ΔN-RGS2 were expressed as GST fusion proteins immobilized on gluthatione-Sepharose 4B beads. Subsequently, these fusion proteins were tested for their interaction with *in vitro* translated [^{35}S]methionine-labeled N-tail of TRPV6 in the presence or absence of 1 mM Ca^{2+}. As shown in Fig. 2, the N-tail of TRPV6 associated with GST-fused RGS2 in a Ca^{2+}-independent fashion whereas no binding between the N-tail of TRPV6 and GST-fused ΔN-RGS2 or GST alone was observed, neither in the presence nor absence of Ca^{2+}.

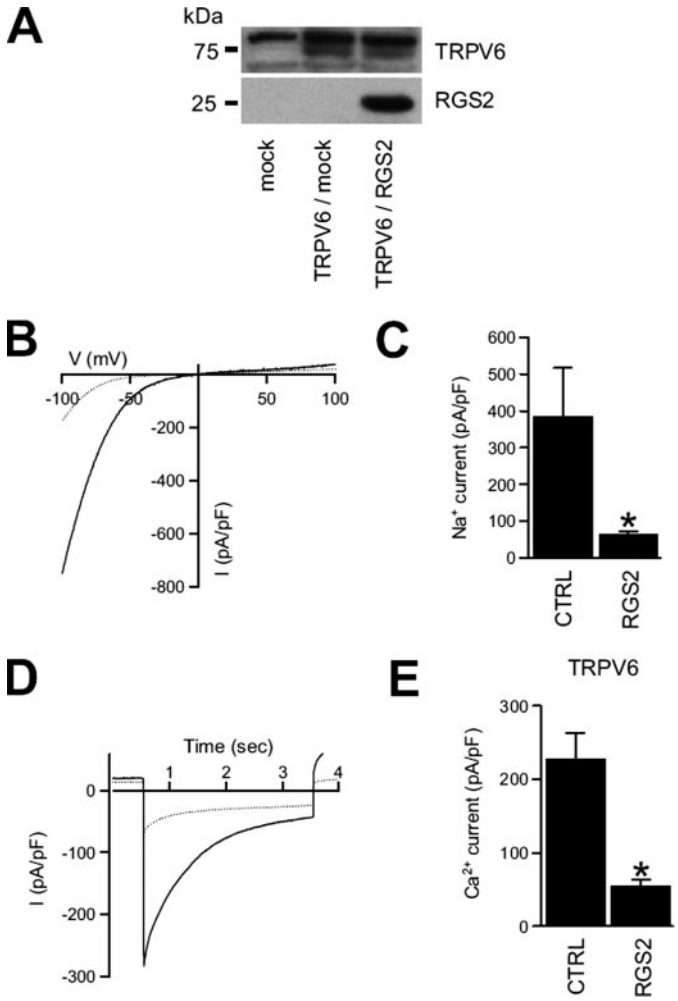

FIGURE 3. **Inhibition of TRPV6-induced Na^+ and Ca^{2+} currents by RGS2.** HEK293 cells were transiently transfected with TRPV6/mock (control (*CTRL*)) or TRPV6/RGS2 and subsequently analyzed by immunoblotting (*A*) and by whole-cell patch clamp. *B*, current-voltage (*I/V*) relations measured from ramp protocol in nominally DVF solution from control (*solid trace*) or TRPV6/RGS2-transfected cells (*dotted trace*). The *I/V* curve shows inward rectification typical for TRPV6 (*solid trace*), which is not changed by co-expressing RGS2 (*dotted trace*). *C*, average Na^+ current density at −80 mV in nominally DVF solution was 384 ± 133 pA/pF for control cells compared with 65 ± 8 pA/pF for TRPV6/RGS2 co-expressing cells ($n = 15$ cells for each condition). *D*, averaged Ca^{2+} currents measured with 10 mM Ca^{2+} in the extracellular solution using the step protocol in control cells (*solid trace*) and TRPV6/RGS2 co-expressing cells (*dotted trace*). *E*, average density of the Ca^{2+} peak current measured as in *D* was 228 ± 35 pA/pF for control compared with 56 ± 8 pA/pF for cells co-transfected with TRPV6 and RGS2 ($n = 15$ cells for each condition). * indicates significant difference ($p < 0.001$).

RGS2 Inhibits Specifically TRPV6 Activity—To study the functional effect of RGS2 binding to TRPV6 the electrophysiological properties of the TRPV6 channel were investigated in the presence of RGS2. Steeply inward rectifying currents carried by Na^+ could be measured in HEK293 cells co-expressing TRPV6 and empty vector (mock) and in cells expressing both TRPV6 and RGS2 (Fig. 3, *A* and *B*). The current carried by Na^+ was significantly reduced in cells expressing both TRPV6 and

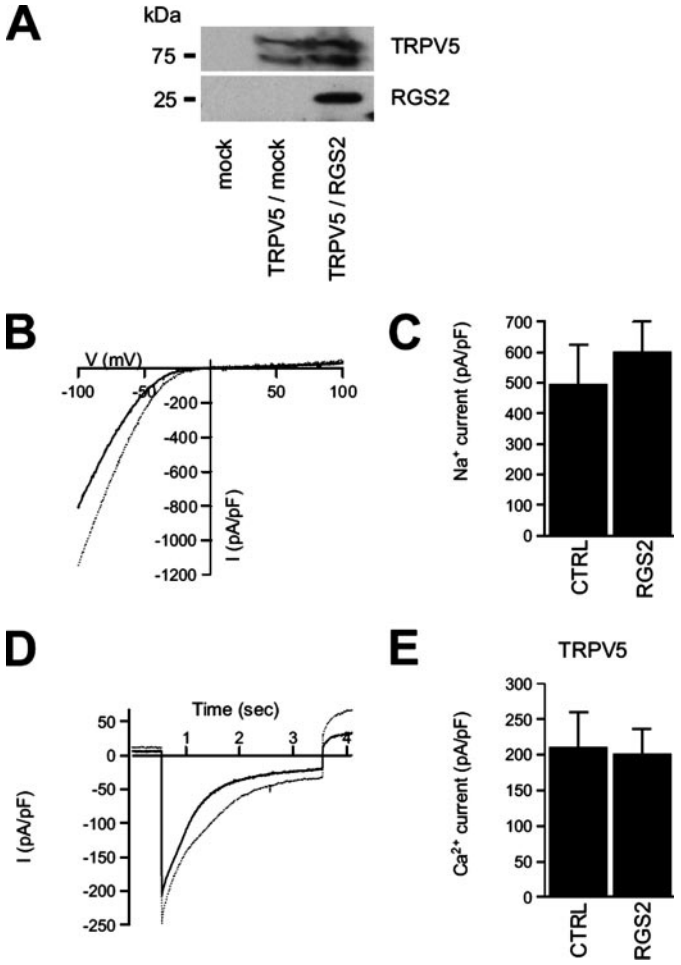

FIGURE 4. **Activity of TRPV5 is not affected by co-expressing RGS2.** HEK293 cells were transiently transfected with TRPV5/mock (control (*CTRL*)) or TRPV5/RGS2 and analyzed using immunoblotting (*A*) and by whole-cell patch clamp. *B*, *I/V* relations measured from ramp protocol in nominally DVF solution in control (*solid trace*) or TRPV5/RGS2-transfected cells (*dotted trace*). *C*, average Na^+ current density at −80 mV in nominally DVF solution was 495 ± 130 pA/pF for control cells compared with 600 ± 100 pA/pF for TRPV5/RGS2 co-expressing cells ($n = 15$ cells for each condition). *D*, averaged Ca^{2+} currents measured with 10 mM Ca^{2+} in the extracellular solution using the step protocol in control cells (*solid trace*) and TRPV5/RGS2-expressing cells (*dotted trace*). *E*, average density of the Ca^{2+} peak current measured as in *D* was 210 ± 50 pA/pF for control compared with 201 ± 35 pA/pF for cells co-transfected with TRPV5 and RGS2 ($n = 15$ cells for each condition).

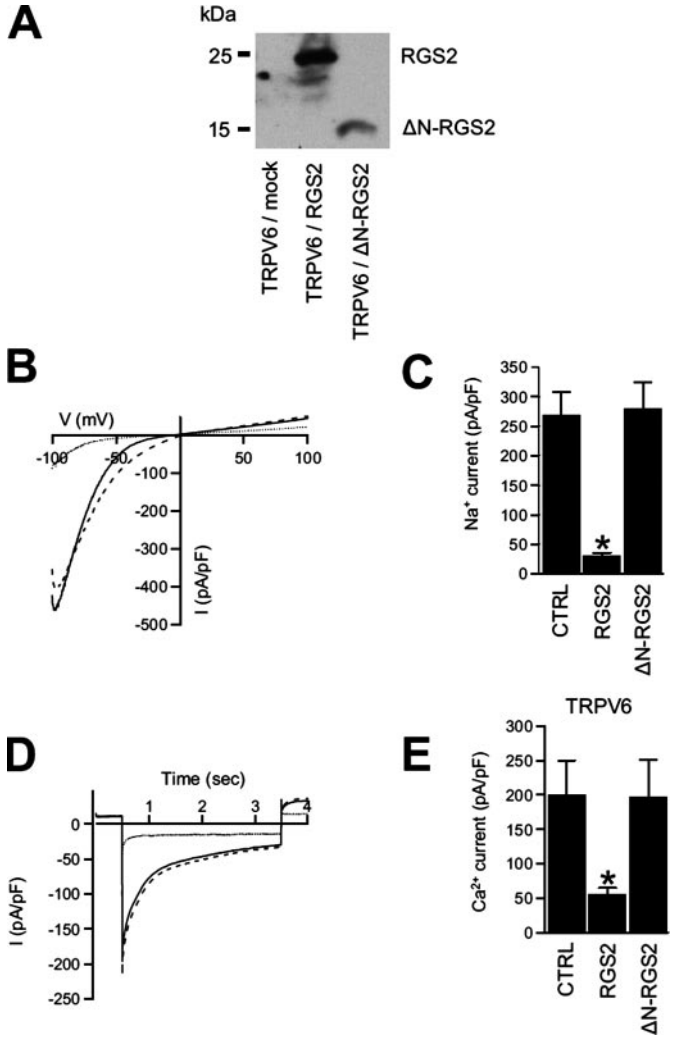

FIGURE 5. **Inhibition of TRPV6-mediated Na^+ and Ca^{2+} currents by RGS2 but not ΔN-RGS2.** HEK293 cells were transiently transfected with TRPV6/mock (control (*CTRL*)) or TRPV6 and RGS2 or ΔN-RGS2 and analyzed using immunoblotting (*A*) and by whole-cell patch clamp. *B*, *I/V* relations measured from ramp protocol in nominally DVF solution from control (*solid trace*), TRPV6/RGS2-transfected cells (*dotted trace*), and TRPV6/ΔN-RGS2-transfected cells (*dashed trace*). *C*, average Na^+ current density at −80 mV in nominally DVF solution was 268 ± 40 pA/pF for control, 30 ± 5 pA/pF for cells transfected with TRPV6 and RGS2, and 280 ± 45 pA/pF for TRPV6/ΔN-RGS2-transfected cells ($n = 10$ cells for each condition). *D*, averaged Ca^{2+} currents measured with 10 mM Ca^{2+} in the extracellular solution using the step protocol in control cells (*solid trace*), TRPV6/RGS2-expressing cells (*dotted trace*), and TRPV6/ΔN-RGS2 co-expressing cells (*dashed trace*). *E*, average density of the Ca^{2+} peak current measured as in *D* was 200 ± 50 pA/pF for control (*CTRL*), 55 ± 10 pA/pF for TRPV6/RGS2 co-expressing cells, and 196 ± 55 pA/pF for TRPV6/ΔN-RGS2 co-expressing cells ($n = 10$ cells for each condition). * indicates significant difference ($p < 0.001$).

RGS2 (Fig. 3, *B* and *C*, $n = 15$ cells, $p < 0.001$). Likewise, RGS2 co-expression significantly reduced the Ca^{2+} current in response to a hyperpolarizing voltage step in TRPV6-expressing cells (Fig. 3, *D* and *E*, $n = 15$ cells, $p < 0.001$), while the Ca^{2+}-dependent inactivation of the currents remained unchanged. In addition, the inhibitory effect of RGS2 on TRPV6-mediated Na^+ and Ca^{2+} currents was studied for its closest relative, TRPV5, during identical experimental conditions. In contrast to TRPV6, RGS2 had no significant effect on Na^+ and Ca^{2+} currents recorded from TRPV5-expressing HEK293 cells (Fig. 4).

TRPV6 Activity Is Inhibited by the NH_2-terminal Domain of RGS2—To test the physiological significance of the NH_2-terminal domain of RGS2 on TRPV6 activity, the electrophysiological properties of TRPV6-mediated currents in HEK293 cells co-expressing either RGS2 or ΔN-RGS2 were determined. Inward rectifying currents carried by Na^+ could be measured in HEK293 cells co-transfected with TRPV6 and ΔN-RGS2 or RGS2 or with TRPV6 and mock (Fig. 5, *A* and *B*). The Na^+ currents were significantly reduced in cells co-expressing TRPV6 with RGS2, whereas cells co-expressing ΔN-RGS2 and TRPV6 did not show this reduction (Fig. 5, *B* and *C*, $n = 10$ cells, $p < 0.001$). Likewise, RGS2 significantly reduced the Ca^{2+} current in response to a hyperpolarizing voltage step in TRPV6-expressing cells (Fig. 5, *D* and *E*, $n = 10$ cells, $p < 0.001$), whereas co-expression of ΔN-RGS2 with TRPV6 had no effect on the TRPV6-mediated current amplitude.

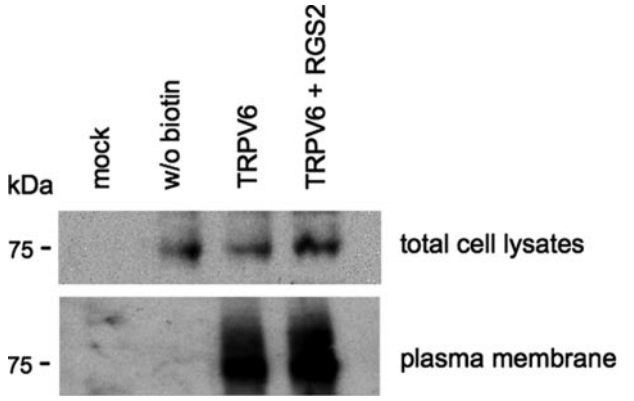

FIGURE 6. **Cell-surface expression of TRPV6.** HEK293 cells were transfected with TRPV6 ± RGS2. The extracellular parts of the proteins were biotinylated, precipitated with neutravidin beads, and immunoblotted for TRPV6. Samples of the lysed cells ("*total cell lysates*," *upper panel*) were immunoblotted in parallel to visualize the amount of expressed proteins. Both TRPV6 alone and TRPV6 with RGS2-transfected cells showed cell surface expression, whereas mock-transfected cells did not ("*plasma membrane*," *lower panel*).

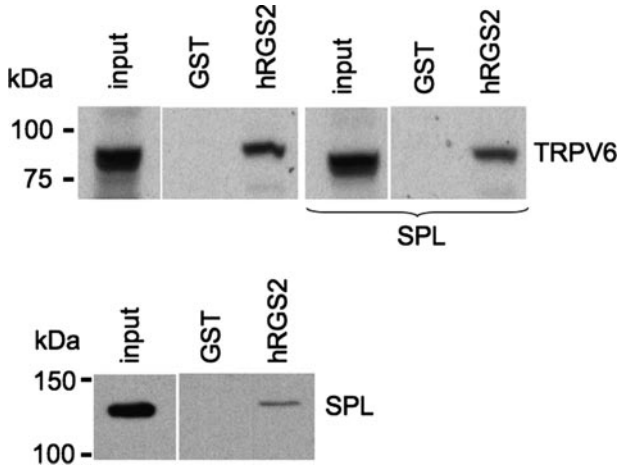

FIGURE 7. **Effect of SPL on the interaction of RGS2 and TRPV6.** Extracts from HEK293 cells transfected with TRPV6 and SPL were used for pull-down assay with GST or GST fused to RGS2. Pulled proteins were analyzed for TRPV6 (*top panel*) and SPL (*lower panel*) expression by immunoblotting.

RGS2 Does Not Affect TRPV6 Abundance at the Plasma Membrane—To investigate whether RGS2 influences trafficking of TRPV6, cell surface expression of TRPV6 in HEK293 cells co-expressing RGS2 and TRPV6 was examined using Sulfo-NHS-LC-LC-Biotin. TRPV6 was detected in total cell lysates of TRPV6-expressing cells as well as in the biotinylated plasma membrane fractions of TRPV6 and TRPV6/RGS2 co-expressing cells (Fig. 6). TRPV6 expression in the biotinylated membrane fraction was not significantly altered by co-expression of RGS2.

TRPV6 Is Independently Regulated from the Scaffolding Protein SPL—The effect of SPL on the interaction of RGS2 with TRPV6 was investigated by GST pulldown assay. Total cell lysates of HEK293 cells transiently transfected with TRPV6, SPL, or TRPV6 and SPL were prepared, and equal amounts of protein were analyzed for the interaction with RGS2. As indicated in Fig. 7, TRPV6 associated with RGS2 both in the presence or absence of SPL. Next, the electrophysiological properties of TRPV6-mediated currents were examined by whole-cell patch clamp in HEK293 cells co-expressing TRPV6 and SPL or TRPV6 and mock. Co-expression of SPL and TRPV6 had no significant effect either on Na^+ or Ca^{2+} currents ($n = 12$ cells for each condition) as depicted in Fig. 8.

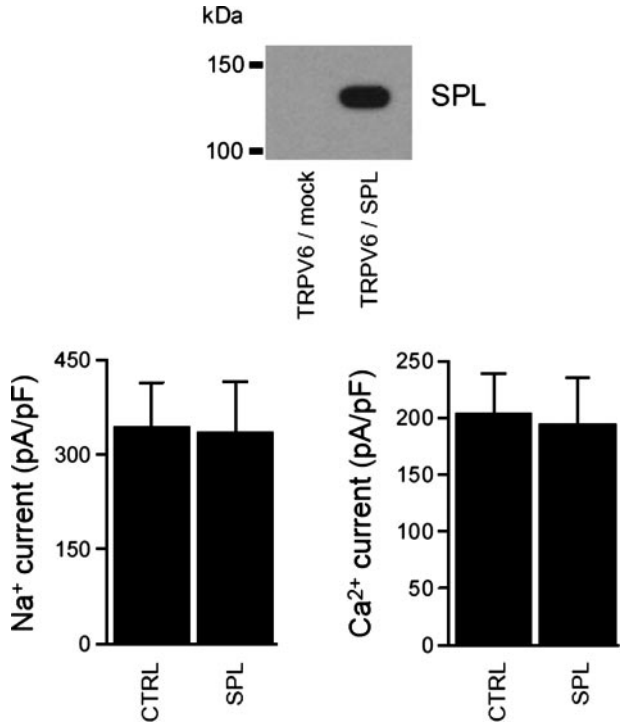

FIGURE 8. **Activity of TRPV6 is not affected by SPL.** HEK293 cells were transiently transfected with TRPV6/mock (control (*CTRL*)) or TRPV6/SPL and analyzed by immunoblotting and by whole-cell patch clamp. Average Na^+ current density measured at −80 mV from the ramp protocol was 344 ± 70 pA/pF for control and 335 ± 80 pA/pF for TRPV6/SPL co-expressing cells and average density of the Ca^{2+} peak current measured from the step protocol was 204 ± 35 pA/pF for control and 195 ± 40 pA/pF for TRPV6/SPL co-expressing cells ($n = 12$ cells for each condition).

DISCUSSION

The present study demonstrates a novel regulatory function of RGS2 by direct inhibition of TRPV6 channel activity at the plasma membrane. This conclusion is based on the following experimental data. First, interaction of RGS2 with TRPV6 specifically inhibits both Na^+ and Ca^{2+} currents through TRPV6 whereas no effect on TRPV5 activity was observed. Second, deletion of the NH_2-terminal domain of RGS2 disrupts the binding with TRPV6 and restores the original electrophysiological properties of the channel. Third, RGS2 expression does not interfere with TRPV6 trafficking from and toward the plasma membrane (to mediate its inhibitory effect on channel activity). Fourth, the multidomain scaffolding protein SPL does not affect binding and electrophysiological properties of TRPV6 in the presence of RGS2. Therefore, our data indicate that TRPV6 activity is regulated by RGS2 without the involvement of GPCR signaling.

We showed that the NH_2-terminal tail of RGS2 is essential for the interaction with and the activity of TRPV6. The NH_2-terminal domain has already been described to be an important regulatory site for RGS2. Together with the "RGS-box" domain, it is necessary for its effector protein interactions, *e.g.* GPCRs and/or auxiliary proteins such as SPL (23, 28, 29). In addition,

the membrane-targeting sequence has also been predicted in this domain (30, 31).

Patch clamp analysis of HEK293 cells transfected with TRPV6 or TRPV5 revealed that specifically TRPV6 activity is inhibited by co-expression of RGS2. Interestingly, an analogous inhibitory mechanism has only been found for calmodulin and TRPV6 (32). Since both Na^+ and Ca^{2+} currents through TRPV6 were inhibited by RGS2, and thus affecting not specifically the Ca^{2+} conductance of the channel, we expected a disturbed TRPV6 trafficking toward the cell surface. In contrast, cell surface biotinylation in TRPV6-expressing HEK293 cells demonstrated that RGS2 does not affect channel expression in the biotinylated fractions. Therefore, the inhibitory effect of RGS2 is presumably mediated directly at the plasma membrane.

RGS2 needs to be recruited toward the cell surface to affect the gating properties of TRPV6. Roy *et al.* (33) showed that G-proteins recruit RGS proteins toward the plasma membrane. In their study, the abundance of RGS2 and RGS4 proteins at the plasma membrane was enhanced when the number of G proteins was increased or when they interacted with their GPCR. Also SPL has been shown to be involved in RGS protein recruitment (23). Investigating the role of SPL provided us with additional evidence for a direct effect of RGS2 on TRPV6 activity. Wang *et al.* (23) showed that SPL is a scavenger of RGS2 which forms a SPL-RGS2 protein complex that regulates Ca^{2+} signaling by binding the third intracellular domain of GPCRs. In their study, the binding of RGS2 with the α-adrenergic receptor was investigated by GST pulldown analysis. The interaction between RGS2 and the α-adrenergic receptor was significantly increased in the presence of SPL. Furthermore, they observed that the inhibitory effect of RGS2 on Ca^{2+}-activated Cl^- currents in parotid duct cells was increased in the presence of SPL. For this reason, we anticipated that SPL could increase the inhibitory effect of endogenously present RGS2 on TRPV6 activity in HEK293 cells when acting via a $G\alpha_q$-coupled GPCR. RGS2 expression was confirmed in HEK293 cells by RT-PCR (data not shown). First, it was demonstrated that SPL does not change TRPV6 expression (Fig. 7, *top panel*). Second, TRPV6-mediated Na^+ and Ca^{2+} currents were not affected by SPL as well (Fig. 8). Therefore, we conclude that the inhibitory effect of RGS2 on TRPV6 activity is independently regulated of a GPCR but is rather mediated by direct interaction of RGS2 and TRPV6.

In conclusion, we have identified RGS2 as a novel regulatory protein specifically inhibiting the activity of the epithelial Ca^{2+} channel TRPV6. Our findings may provide insight in the direct regulation of different TRP channels by interacted proteins at the plasma membrane.

Acknowledgments—We thank Dr. K. M. Druey (Molecular Signal Transduction Section, Laboratory of Allergic Diseases, NIAID, National Institutes of Health, Bethesda, MD) for kindly providing the RGS2 antibody and J. A. Janssen for excellent technical assistance.

REFERENCES

1. Birnbaumer, L., Yildirim, E., and Abramowitz, J. (2003) *Cell Calcium* **33,** 419–432
2. Clapham, D. E. (2003) *Nature* **426,** 517–524
3. Montell, C. (2003) *Cell Calcium* **33,** 409–417
4. Putney, J. W., Jr. (2003) *Cell Calcium* **34,** 339–344
5. Montell, C., Birnbaumer, L., and Flockerzi, V. (2002) *Cell* **108,** 595–598
6. Hoenderop, J. G., Vennekens, R., Muller, D., Prenen, J., Droogmans, G., Bindels, R. J., and Nilius, B. (2001) *J. Physiol. (Lond.)* **537,** 747–761
7. Pedersen, S. F., Owsianik, G., and Nilius, B. (2005) *Cell Calcium* **38,** 233–252
8. Voets, T., Janssens, A., Prenen, J., Droogmans, G., and Nilius, B. (2003) *J. Gen. Physiol.* **121,** 245–260
9. Voets, T., Janssens, A., Droogmans, G., and Nilius, B. (2004) *J. Biol. Chem.* **279,** 15223–15230
10. Peng, J. B., Chen, X. Z., Berger, U. V., Vassilev, P. M., Tsukaguchi, H., Brown, E. M., and Hediger, M. A. (1999) *J. Biol. Chem.* **274,** 22739–22746
11. Nijenhuis, T., Hoenderop, J. G., van der Kemp, A. W., and Bindels, R. J. (2003) *J. Am. Soc. Nephrol.* **14,** 2731–2740
12. Wissenbach, U., Niemeyer, B. A., Fixemer, T., Schneidewind, A., Trost, C., Cavalie, A., Reus, K., Meese, E., Bonkhoff, H., and Flockerzi, V. (2001) *J. Biol. Chem.* **276,** 19461–19468
13. den Dekker, E., Hoenderop, J. G., Nilius, B., and Bindels, R. J. (2003) *Cell Calcium* **33,** 497–507
14. Hoenderop, J. G., Nilius, B., and Bindels, R. J. (2005) *Physiol. Rev.* **85,** 373–422
15. van de Graaf, S. F., Chang, Q., Mensenkamp, A. R., Hoenderop, J. G., and Bindels, R. J. (2006) *Mol. Cell. Biol.* **26,** 303–312
16. van de Graaf, S. F., Hoenderop, J. G., Gkika, D., Lamers, D., Prenen, J., Rescher, U., Gerke, V., Staub, O., Nilius, B., and Bindels, R. J. (2003) *EMBO J.* **22,** 1478–1487
17. van de Graaf, S. F., Hoenderop, J. G., van der Kemp, A. W., Gisler, S. M., and Bindels, R. J. (2006) *Pfluegers Arch.* **452,** 407–417
18. Erler, I., Hirnet, D., Wissenbach, U., Flockerzi, V., and Niemeyer, B. A. (2004) *J. Biol. Chem.* **279,** 34456–34463
19. Mosavi, L. K., Cammett, T. J., Desrosiers, D. C., and Peng, Z. Y. (2004) *Protein Sci.* **13,** 1435–1448
20. De Vries, L., Zheng, B., Fischer, T., Elenko, E., and Farquhar, M. G. (2000) *Annu. Rev. Pharmacol. Toxicol.* **40,** 235–271
21. Abramow-Newerly, M., Roy, A. A., Nunn, C., and Chidiac, P. (2006) *Cell. Signal.* **18,** 579–591
22. Nilius, B., Prenen, J., Hoenderop, J. G., Vennekens, R., Hoefs, S., Weidema, A. F., Droogmans, G., and Bindels, R. J. (2002) *J. Biol. Chem.* **277,** 30852–30858
23. Wang, X., Zeng, W., Soyombo, A. A., Tang, W., Ross, E. M., Barnes, A. P., Milgram, S. L., Penninger, J. M., Allen, P. B., Greengard, P., and Muallem, S. (2005) *Nat. Cell Biol.* **7,** 405–411
24. van Abel, M., Hoenderop, J. G., Dardenne, O., St Arnaud, R., Van Os, C. H., Van Leeuwen, H. J., and Bindels, R. J. (2002) *J. Am. Soc. Nephrol.* **13,** 2102–2109
25. Vennekens, R., Hoenderop, J. G., Prenen, J., Stuiver, M., Willems, P. H., Droogmans, G., Nilius, B., and Bindels, R. J. (2000) *J. Biol. Chem.* **275,** 3963–3969
26. Chang, Q., Hoefs, S., van der Kemp, A. W., Topala, C. N., Bindels, R. J., and Hoenderop, J. G. (2005) *Science* **310,** 490–493
27. Ross, E. M., and Wilkie, T. M. (2000) *Annu. Rev. Biochem.* **69,** 795–827
28. Bernstein, L. S., Ramineni, S., Hague, C., Cladman, W., Chidiac, P., Levey, A. I., and Hepler, J. R. (2004) *J. Biol. Chem.* **279,** 21248–21256
29. Hague, C., Bernstein, L. S., Ramineni, S., Chen, Z., Minneman, K. P., and Hepler, J. R. (2005) *J. Biol. Chem.* **280,** 27289–27295
30. Heximer, S. P., Lim, H., Bernard, J. L., and Blumer, K. J. (2001) *J. Biol. Chem.* **276,** 14195–14203
31. Kehrl, J. H., and Sinnarajah, S. (2002) *Int. J. Biochem. Cell Biol.* **34,** 432–438
32. Lambers, T. T., Weidema, A. F., Nilius, B., Hoenderop, J. G., and Bindels, R. J. (2004) *J. Biol. Chem.* **279,** 28855–28861
33. Roy, A. A., Lemberg, K. E., and Chidiac, P. (2003) *Mol. Pharmacol.* **64,** 587–593

RGS2 Inhibits the Epithelial Ca^{2+} Channel TRPV6

Joost P. Schoeber, Catalin N. Topala, Xinhua Wang, Robin J. Diepens, Tim T. Lambers, Joost G. Hoenderop and René J. Bindels

J. Biol. Chem. 2006, 281:29669-29674.
doi: 10.1074/jbc.M606233200 originally published online August 8, 2006
